JACC: BASIC TO TRANSLATIONAL SCIENCE
VOL. 2, NO. 1, 2017
ISSN 2452-302X
http://dx.doi.org/10.1016/j.jacbts.2016.09.007

PRECLINICAL RESEARCH

Renal Denervation Reduces Pulmonary Vascular Remodeling and Right Ventricular Diastolic Stiffness in Experimental Pulmonary Hypertension

Denielli da Silva Gonçalves Bos, MSc,[a,b] Chris Happé, MSc,[a,b] Ingrid Schalij, BSc,[a,b] Wioletta Pijacka, PhD,[c] Julian F.R. Paton, PhD,[c] Christophe Guignabert, PhD,[d,e] Ly Tu, PhD,[d,e] Raphaël Thuillet, BSc,[d,e] Harm-Jan Bogaard, MD, PhD,[a] Albert C. van Rossum, MD, PhD,[f] Anton Vonk-Noordegraaf, MD, PhD,[a] Frances S. de Man, PhD,[a,b] M. Louis Handoko, MD, PhD[b,f]

VISUAL ABSTRACT

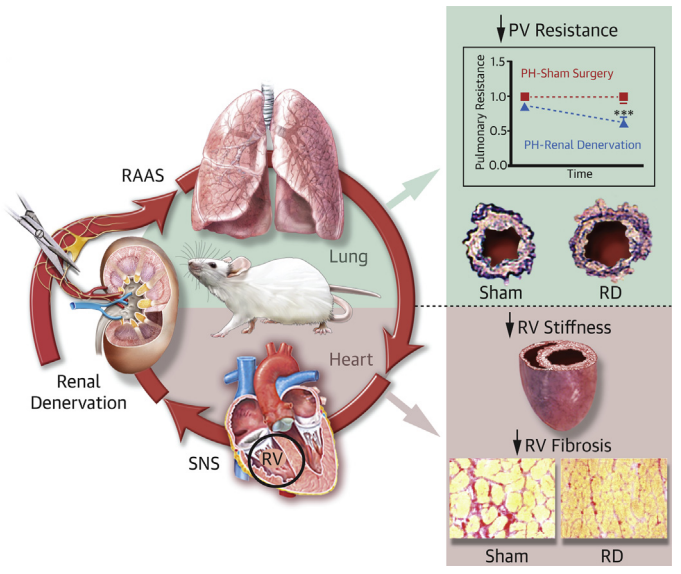

da Silva Gonçalves Bos, D. et al. J Am Coll Cardiol Basic Trans Science. 2017;2(1):22-35.

HIGHLIGHTS

- **Neurohormonal dysfunction (increased sympathetic nervous system and renin angiotensin-aldosterone system) play an important role in pulmonary hypertension progression.**
- **In this proof-of-concept study we demonstrated in 2 pulmonary hypertension rat models that renal denervation therapy improved pulmonary vascular remodeling, lowered right ventricular afterload, and decreased right ventricular stiffness.**
- **Renal denervation effects may be associated with a suppression of the renin-angiotensin-aldosterone system.**

From the [a]Department of Pulmonology, VU University Medical Center, Institute for Cardiovascular Research, Amsterdam, the Netherlands; [b]Department of Physiology VU University Medical Center, Institute for Cardiovascular Research, Amsterdam, the Netherlands; [c]School of Physiology, Pharmacology & Neuroscience, Biomedical Sciences, University of Bristol, Bristol, United Kingdom; [d]University of Paris-Sud, Faculté de Médecine, Université Paris-Saclay, Le Kremlin Bicêtre, France; [e]INSERM UMR_S 999, Hôpital Marie Lannelongue, Le Plessis-Robinson, France; and the [f]Department of Cardiology, VU University Medical Center, Institute for Cardiovascular Research, Amsterdam, the Netherlands. Dr. da Silva Gonçalves Bos is supported by the Science Without Borders grant, Conselho Nacional de Desenvolvimento Científico e Tecnológico (CNPq-Brasil). Dr. Paton is supported by the British Heart Foundation. Drs. Vonk-Noordegraaf, Bogaard, and de Man are supported by the Netherlands CardioVascular Research Initiative grant (2012-08) awarded to the Phaedra Consortium. Dr. de Man received a VENI grant from the Netherlands Organization for Scientific Research (NWO 916.14.099); and is further supported by L'Oréal/UNESCO for Women in Science and Netherlands Institute for Advanced Studies (NIAS); the American Thoracic Society (ATS) (Jerry Wojciechowski Memorial Pulmonary Hypertension Research Grant); and the European Respiratory Society. Dr. Handoko has received a MD/PhD grant by the Institute for Cardiovascular Research (ICaR-VU). All other authors have reported that they have no relationships relevant to the contents of this paper to disclose.

SUMMARY

Neurohormonal overactivation plays an important role in pulmonary hypertension (PH). In this context, renal denervation, which aims to inhibit the neurohormonal systems, may be a promising adjunct therapy in PH. In this proof-of-concept study, we have demonstrated in 2 experimental models of PH that renal denervation delayed disease progression, reduced pulmonary vascular remodeling, lowered right ventricular afterload, and decreased right ventricular diastolic stiffness, most likely by suppression of the renin-angiotensin-aldosterone system. (J Am Coll Cardiol Basic Trans Science 2017;2:22–35) © 2017 The Authors. Published by Elsevier on behalf of the American College of Cardiology Foundation. This is an open access article under the CC BY-NC-ND license (http://creativecommons.org/licenses/by-nc-nd/4.0/).

ABBREVIATIONS AND ACRONYMS

AT1 = angiotensin II type 1

Ea = right ventricular afterload

Eed = right ventricular stiffness

Ees = right ventricular contractility

MCT = monocrotaline model

PH = pulmonary hypertension

RAAS = renin angiotensin-aldosterone system

RD = renal denervation

SNS = sympathetic nervous system

SuHx = sugen combined with hypoxia model

Pulmonary hypertension (PH) is a fatal disease characterized by excessive pulmonary vascular remodeling and increased right ventricular (RV) afterload, subsequently leading to RV maladaptive remodeling and failure (1,2).

Neurohormonal mediators, such as the sympathetic nervous system (SNS) and renin angiotensin-aldosterone system (RAAS) are involved in the progression of PH and may contribute to pulmonary vascular remodeling and RV dysfunction (3–6). Increased levels of SNS activity have been reported in PH patients (7,8) and are associated with disease progression and prognosis (9). Previously reported evidence by our group and others showed that systemic (10) and local (11) RAAS activities are increased in PH patients and are also associated with disease progression (4). Additionally, we demonstrated that chronic angiotensin II type 1 (AT1)-receptor blocker treatment delayed disease progression, reduced pulmonary vascular remodeling, and improved RV diastolic function in a PH animal model (4). Furthermore, previous studies in experimental PH provided evidence that modulation of the sympathetic system improved RV systolic function (12,13) and pulmonary vascular remodeling (12,14). Therefore, targeting the RAAS and SNS could be a promising therapy in PH (1,3,5).

SEE PAGE 36

In this context, renal denervation (RD) might be pertinent. RD aims to abolish afferent and efferent renal nerve signaling (15–17). Afferent renal nerve activation is sympathoexcitatory (18,19), whereas renal efferent nerve activation results in vasoconstriction, sodium retention, release of renin from the juxtaglomerular cells, and contributes to angiotensin II and aldosterone production (20,21), both of which exacerbate PH. In the present study, we investigate the effect of RD treatment on pulmonary vascular remodeling and cardiac function in 2 well-established PH animal models (4,22,23).

METHODS

All experiments were approved by the Institutional Animal Care and Use Committee of the VU University, Amsterdam, the Netherlands (FYS 13-05 and 14-10) and performed according to the Declaration of Helsinki conventions for the use and care of animals.

EXPERIMENTAL PH. In this study we investigated the effects of RD-therapy in 2 PH animal models: monocrotaline (MCT) and sugen 5416 combined with chronic hypoxia (SuHx) (4,22,23). PH status was confirmed by echocardiography at week 2 (MCT model) and week 6 (SuHx model); at this point animals were randomized to sham surgery or RD surgery. At end-of-study (week 6 for MCT; week 10 for SuHx, or when animals manifest signs of right heart failure), echocardiography and RV catheterization with pressure-volume analyses were performed. An overview flow of the study design can be found in Supplemental Figure S1A and S1B (4,13).

SURGICAL RD. Thirty minutes before anesthesia (isoflurane induction: 4.0% in 1:1 O_2/air mix; maintenance: 2.0% in 1:1 O_2/air mix), rats received an injection of analgesia (buprenorphine; 0.1 mg/kg subcutaneously). Bilateral flank incisions were performed and the kidneys were approached retroperitoneally. The renal arteries and veins were stripped from the adventitia. All visible renal nerve bundles

All authors attest they are in compliance with human studies committees and animal welfare regulations of the authors' institutions and Food and Drug Administration guidelines, including patient consent where appropriate. For more information, visit the *JACC: Basic to Translational Science* author instructions page.

Manuscript received August 29, 2016; revised manuscript received September 17, 2016, accepted September 20, 2016.

were cut under a dissection microscope (25X) and the vessels were coated with a solution of 10% phenol in ethanol (24). In the sham group, the same surgical procedure was performed, but renal nerves remained intact and no phenol solution was used. Analgesic (carprofen; 4.0 mg/kg subcutaneously) was used directly after surgery, and 24 h and 48 h after the procedure. The animals recovered from the surgery within 1 week. The efficacy of this procedure was evaluated by measuring renal tissue norepinephrine content, assessed by enzyme-linked immunosorbent assay (Alpco Diagnostics, Salem, New Hampshire, No 17-NORHU-E01-RES), and normalized to protein concentration.

RV PRESSURE-VOLUME RELATIONSHIPS. RV open-chest catheterization was performed using a combined pressure-volume catheter (SPR-869, Millar Instruments, Houston, Texas). Details regarding the RV catheterization can be found online in the Supplemental Material and Methods section. Stroke volume (in relative volume units) obtained from the conductance catheter was calibrated using the echocardiogram stroke volume (in ml). Using custom-made algorithms (programmed in MATLAB 2007b, The MathWorks, Natick, Massachusetts) RV (peak-) systolic pressures and RV end-diastolic pressures were automatically determined from RV catheterization steady-state measurements, as well as arterial elastance (Ea), a measurement of RV afterload (25). From vena cava occlusion, end-systolic elastance (Ees) (RV contractility) and end-diastolic elastance (Eed) (RV stiffness) were determined (13). These parameters represent the slope of end-systolic and end-diastolic pressure-volume relationships, and are considered load-independent measurements for cardiac contractility (Ees) and stiffness (Eed) (26). The ratio Ees/Ea was calculated, and it represents the RV-arterial coupling.

HISTOMORPHOLOGY OF HEART AND LUNGS. After hemodynamic evaluation, rats were euthanized by exsanguination under isoflurane. Heart, lungs, and other major organs were harvested. Cardiomyocyte cross-sectional area, cardiac fibrosis, and relative wall thickness of pulmonary arterioles were determined.

CARDIOMYOCYTE CROSS-SECTIONAL AREA. Hematoxylin and eosin–stained cardiac cryosections (5 μm) were used to determine left ventricular (LV) and RV cardiomyocyte cross-sectional area (CSA). Cardiomyocyte size for each ventricle was expressed as the average CSA of minimally 20 transversally cut cardiomyocytes at the level of the nucleus, randomly distributed over the ventricles.

CARDIAC FIBROSIS. The combination of Picrosirius red staining (5 μm) and polarized light was used for analysis of cardiac fibrosis (27). LV and RV fibrosis were expressed as the percentage tissue area positive for collagen, measured over minimally 5 random areas per ventricle.

RELATIVE WALL THICKNESS OF PULMONARY ARTERIOLES. Lung cryosections (5 μm) were stained with Elastica van Gieson for morphometric analysis of vascular dimensions. Minimally, 50 transversal pulmonary arterioles with an outer diameter between 25 μm and 100 μm were randomly measured over the lungs. Media and intima wall thickness were measured in duplicate as described previously (23).

IMMUNOFLUORESCENCE AND PROTEIN EXPRESSION. AT1-receptor, mineralocorticoid receptor (MR) density, and proliferation activity (Ki67) were evaluated by immunofluorescence in the pulmonary vasculature. In addition, AT1 and MR receptor expression were measured in the RV homogenates by Western blot (Supplemental Material and Methods).

STATISTICAL ANALYSIS. Statistical analyses were performed using Prism for Windows (GraphPad 6 Software, San Diego, California). Data are presented as mean ± SEM. Values of $p < 0.05$ were considered significant. All variables were visually checked for normal distribution by appreciation of the histogram and comparing mean versus median value (which should be about the same) and standard deviation (SD) versus the mean ($2 \bullet SD < mean$). Data that failed these criteria were log-transformed and these log-transformed data were again visually checked using the same criteria. For the MCT model, the following variables were log-transformed: Eed, percentage of open/fully occluded vessels, immunofluorescence for AT1 and MR receptors, and Western blot analysis for MR receptor. For the SuHx-model, the following variables were log-transformed: Ees, percentage of open/fully occluded vessels, and immunofluorescence for Ki67. Comparison between echocardiography analyses before and after RD treatment was performed by 2-way analysis of variance (ANOVA) for repeated measurements followed by the Bonferroni post-hoc test. One-way ANOVA with Bonferroni post-hoc comparison between sham and RD groups was used for pressure-volume relationships, autopsy data, and protein analyses. Histology data were analyzed using multilevel analysis to correct for nonindependence of successive measurements per animal (MLwiN 2.02.03, Center for Multilevel Modeling, Bristol, United Kingdom) (4,13,22,28,29).

TABLE 1 Hemodynamic Data for the Monocrotaline Model

	Control (n = 5)	MCT-Sham (n = 9)	MCT-RD (n = 9)	p Value	
				Control vs. MCT	MCT vs. RD
RV end-systolic pressure (mm Hg)	27 ± 2.5	66 ± 2.9	61 ± 2.3	<0.001	0.35
RV end-diastolic pressure (mm Hg)	2.8 ± 0.6	3.9 ± 0.6	3.3 ± 0.3	0.57	0.97
dP/dt maximum (mm Hg/s)	1,681 ± 218	2,732 ± 170	2,554 ± 126	<0.001	0.42
dP/dt minimum (mm Hg/s)	-1,293 ± 174	-2,366 ± 141	-2,405 ± 100	<0.001	0.83
Tau (ms)	11 ± 2.5	13 ± 1.0	12 ± 0.4	0.32	0.46
Systolic blood pressure (mm Hg)	102 ± 6.6	88 ± 3.1	75 ± 3.3	0.15	0.03
Diastolic blood pressure (mm Hg)	67 ± 7.9	65 ± 2.6	51 ± 3.2	>0.999	0.03
SVR (mm Hg·min·ml^{-1})	0.6 ± 0.1	1.9 ± 0.3	1.1 ± 0.1	0.002	0.01
Heart rate (beats/min)	300 ± 11.4	317 ± 5.5	300 ± 13.7	>0.999	0.30

Values are mean ± SEM. One-way ANOVA followed by Bonferroni correction.
MCT = monocrotaline; RD = renal denervation; RV = right ventricle; SVR = systemic vascular resistance; Tau = isovolumic relaxation constant.

RESULTS

GENERAL HEMODYNAMIC EFFECTS OF RD IN EXPERIMENTAL PH. All MCT rats and 1 SuHx rat developed early signs of heart failure at week 4 and week 8, respectively. The efficacy of RD was confirmed by a significant reduction of norepinephrine levels in kidney tissue (Supplemental Figures S2A and S2B). Renal norepinephrine levels were reduced by 97% (MCT) and 81% (SuHx).

However, measured under anesthesia, the systolic and diastolic blood pressures and systemic vascular resistance were significantly reduced after RD (**Tables 1 and 2**), whereas no effect in heart rate or in RV end-systolic pressure were observed after RD treatment (**Tables 1 and 2**). Other than the hypotensive effect of RD therapy, no macroscopic kidney damage, kidney mass (Supplemental Tables S1 and S2), or signs of animal discomfort were observed.

Before surgery was performed, PH development in both models was confirmed by echocardiography (Supplemental Tables S3 and S4, **Figure 1**). After RD surgery, echocardiographic measurements showed a significant delay in disease progression in RD-PH rats (**Figure 1**). Pulmonary vascular resistance and RV wall thickness (**Figures 1A to 1D**) was significantly reduced in both models after RD treatment in comparison to the sham group. However, no significant effects in RV end-diastolic diameter, tricuspid annular plane systolic excursion, and cardiac output were observed (**Figures 1E to 1J**).

RD REDUCED RV AFTERLOAD AND RV DIASTOLIC STIFFNESS. To assess the effect of RD on load-independent parameters of RV function, we performed RV pressure-volume analyses at the end of the study (representative pressure-volumes can be found in **Figures 2A to 2C and 3A to 3C**). RD significantly reduced RV afterload (Ea) (**Figures 2D and 3D**) and RV stiffness (Eed) (**Figures 2F and 3F**) without significant effect in RV relaxation (dP/dt min and Tau) (**Tables 1 and 2**). Although not statistically significant, we observed a minor reduction in RV contractility

TABLE 2 Hemodynamic Data for the Sugen + Hypoxia Model

	Control (n = 6)	SuHx-sham (n = 10)	SuHx-RD (n = 10)	p Value	
				Control vs. SuHx	SuHx vs. RD
RV end-systolic pressure (mm Hg)	24 ± 0.93	60 ± 3.3	56 ± 3.3	<0.001	0.39
RV end-diastolic pressure (mm Hg)	1.9 ± 0.09	2.7 ± 0.4	3.3 ± 0.4	0.56	0.22
dP/dt maximum (mm Hg/s)	1,149 ± 40	2,515 ± 142	2,733 ± 210	<0.001	0.34
dP/dt minimum (mm Hg/s)	-953 ± 43	-2,092 ± 146	-2,267 ± 202	<0.001	0.43
Tau (ms)	5.1 ± 0.45	10.1 ± 0.79	10.7 ± 0.88	<0.001	0.63
Systolic blood pressure (mm Hg)	86 ± 3.5	90 ± 6.71	80 ± 4.1	>0.999	0.17
Diastolic blood pressure (mm Hg)	59 ± 3.2	66 ± 7.1	54 ± 3.9	>0.999	0.12
SVR (mm Hg·min·ml^{-1})	0.7 ± 0.03	1.3 ± 0.2	0.9 ± 0.09	0.01	0.03
Heart rate (beats/min)	261 ± 8.5	274 ± 10.1	249 ± 9.5	>0.999	0.21

Values are mean ± SEM. One-way ANOVA followed by Bonferroni correction.
SuHx = sugen + hypoxia; other abbreviations as in **Table 1**.

FIGURE 1 Renal Denervation Significantly Delayed Disease Progression in Both Animal Models

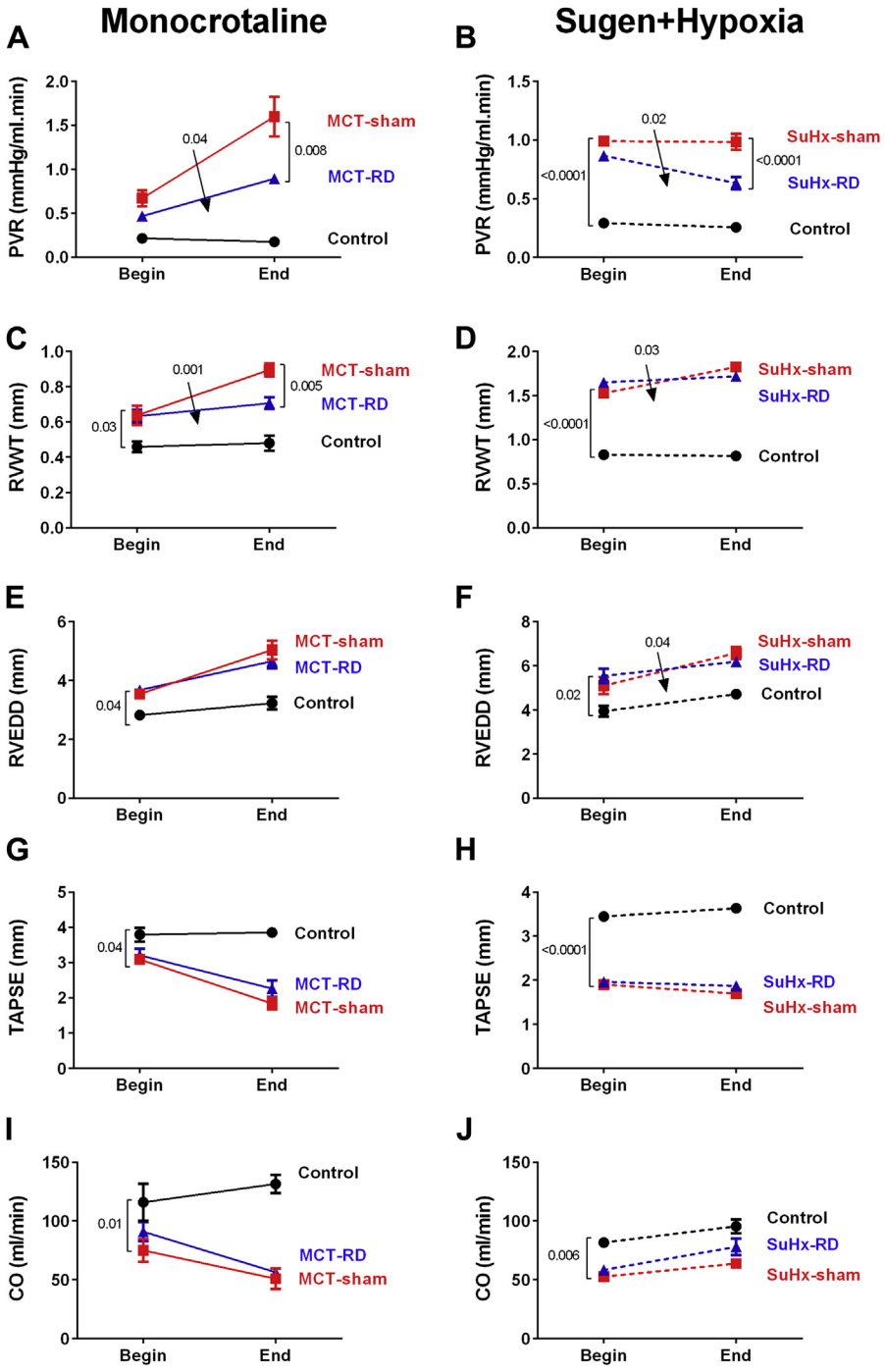

RD reduced significant pulmonary vascular resistance (**A**: MCT model; **B**: SuHx model). In addition, RD delayed the RV hypertrophy (**C:** MCT; **D:** SuHx). No changes were observed in RV end-diastolic diameter (**E:** MCT; **F:** SuHx) and in RV function (**G:** MCT; **H:** SuHx) or in cardiac output (**I:** MCT; **J:** SuHx). **On the right side:** Control: n = 5, MCT-sham: n = 9, and MCT-RD: n = 9. **On the left side:** Control: n = 6, SuHx-sham: n = 10, and SuHx-RD: n = 10. Data presented as mean ± SEM. Two-way ANOVA for repeated measurements followed by Bonferroni correction. **Arrows** indicate the interaction from 2-way ANOVA. ANOVA = analysis of variance; CO = cardiac output; MCT = monocrotaline; PVR = pulmonary vascular resistance; RD = renal denervation; RV = right ventricular; RVEDD = right ventricle end-diastolic diameter; RVWT= right ventricle wall thickness; SuHx = sugen + hypoxia; TAPSE = tricuspid annular plane systolic excursion.

FIGURE 2 Pressure-Volume Analyses in Monocrotaline Model

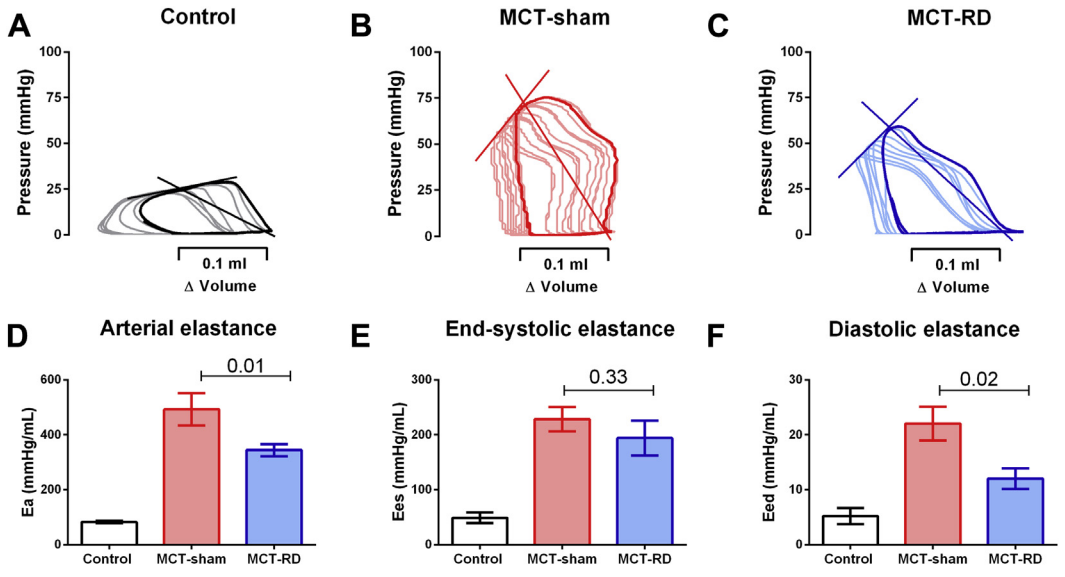

Representative examples of pressure-volume relationship for control, MCT-sham, and MCT-RD groups **(A to C)**. RD significantly reduced RV afterload **(D)**, without affecting RV contractility **(E)** and reduced RV stiffness **(F)**. Control: n = 5, MCT-sham: n = 9, and MCT-RD: n = 9. Data are presented as mean ± SEM. One-way ANOVA followed by Bonferroni correction. Ea = RV afterload; Eed = RV stiffness; Ees = RV contractility; other abbreviations as in Figure 1.

(Ees) (Figures 2E and 3E) and a minor increase in RV arterial coupling after RD (Ees/Ea-MCT: 0.60 ± 0.05 vs. 0.50 ± 0.10; p = 0.45; SuHx: 0.80 ± 0.09 vs. 0.60 ± 0.07; p = 0.13) .

RD REDUCED PULMONARY VASCULAR AND RV REMODELING. Analysis of pulmonary vascular and RV morphometry was performed to confirm changes in RV afterload and remodeling at the tissue level. Histological analyses from the relative wall thickness of pulmonary arterioles indicated a significant reduction in media wall thickness in both models (Figures 4C and 4D), and reduced intima wall thickness in the SuHx model (Figure 4E). Moreover, RD treatment decreased the formation of occlusive vascular lesions in both PH models (Figures 4F and 4G).

RV cardiomyocyte CSA was significantly reduced in both models due to RD (Figure 5); however, no effect on LV cardiomyocyte CSA was observed (Supplemental Tables S1 and S2). Furthermore, we observed a significant reduction of RV fibrosis in the SuHx-RD group (Figure 5F), but this finding was not significant neither in the MCT model (Figure 5E) nor in the LV from both models (Supplemental Tables S1 and S2).

AT1 RECEPTOR EXPRESSION AND CELL PROLIFERATION WERE REDUCED AFTER RD. To further investigate the effects of RD on pulmonary vascular remodeling, we assessed changes in local AT1 receptor and cell proliferation (Ki67) by immunofluorescence staining of pulmonary arterioles. After RD therapy, the staining demonstrated a reduction of AT1 receptor density in pulmonary arterial smooth muscle cells (Figures 6A to 6D) and the rate of proliferative cells (Figures 7A to 7D) in both PH rat models. Moreover, to investigate the effects of RD on the RV remodeling, we also assessed changes in AT1 receptor expression in RV homogenates. Western blot analyses of RV homogenates revealed reduced expression of the AT1 receptor in the MCT model (Figure 8A), but not in the SuHx model (Figure 8B). These data might suggest that the effects of RD on RV afterload and pulmonary vascular remodeling could be associated with reduced AT1 receptor density in pulmonary arterial smooth muscle cells.

MR EXPRESSION WAS REDUCED AFTER RD. Besides changes in angiotensin II signaling, reduced aldosterone signaling may also contribute to the beneficial effects of RD. Aldosterone can promote vascular and RV remodeling via MR binding. Here we measured MR density in lungs by immunofluorescence and MR expression in RV by Western blot. We observed that RD was able to reduced local MR density in the pulmonary vasculature in the SuHx model (Figures 6E to 6H).

FIGURE 3 Pressure-Volume Analyses in Sugen + Hypoxia Model

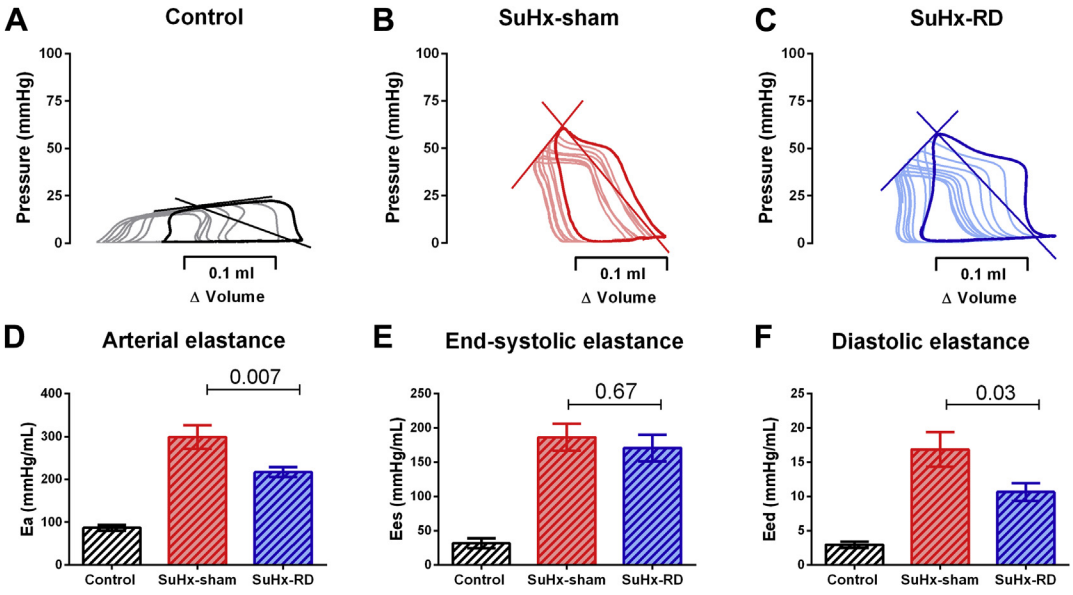

Representative examples of pressure-volume relationship for control, SuHx-sham and SuHx-RD groups **(A to C)**. RD significantly reduced Ea **(D)**, without affecting Ees **(E)** and reduced Eed **(F)**. Control: n = 6, SuHx-sham: n = 10, SuHx-RD: n = 10. Data are presented as mean ± SEM. One-way ANOVA followed by Bonferroni correction. Abbreviations as in Figures 1 and 2.

Moreover, RD reduced the MR expression in RV homogenates of both PH rat models (**Figures 8C and 8D**). This might suggest that observed changes in RV diastolic stiffness, RV hypertrophy, and fibrosis could be related to reduced local MR-expression.

DISCUSSION

This study investigated the effects of RD on pulmonary vascular remodeling and RV function. Using 2 well-established PH animal models, MCT and SuHx, we demonstrated that: 1) RD delayed disease progression; 2) RD reduced RV afterload and pulmonary vascular remodeling; 3) RD reduced diastolic stiffness, hypertrophy, and fibrosis of the RV; and 4) Beneficial effects of RD could be associated with RAAS suppression.

RD DELAYED PH PROGRESSION AND REDUCED PULMONARY VASCULAR REMODELING. RD is a widely studied novel treatment modality for resistant systemic hypertension. By applying radiofrequency energy along the length of the main renal arteries to ablate the renal nerves, sympathetic overactivation (24,30) and renin release of the kidney (31) can be prevented in humans.

Recent studies have revealed that both the SNS as well as the RAAS are upregulated and closely associated to disease progression in PH patients (4). However, whether RD may be clinically beneficial in PH patients is currently unclear.

Promising beneficial effects of RD have been published recently in a canine model for PH (32,33). In contrast to our study, they initiated treatment before PH development, which limits the clinical translation of their findings. Therefore, we performed a therapeutic study with RD in 2 well-established PH animal models, the MCT and SuHx rat models. We demonstrated that chronic RD treatment delayed disease progression and reduced pulmonary vascular remodeling and proliferation in both animal models. Previous data from our group revealed that both systemic as well as local RAAS activity is increased in PH patients and closely related to disease progression (4). Specifically, altered expression of the AT1 receptor was identified as a key regulator of increased RAAS in the pulmonary vasculature because its acute and chronic inhibition resulted in marked improvements in pulmonary vascular remodeling and smooth muscle cell proliferation (4). Therefore, to investigate whether changes in local RAAS could explain the delayed disease progression and pulmonary vascular remodeling after RD, we assessed AT1 receptor density and cell proliferation in both models. Intriguingly, RD was able to reduce

FIGURE 4 **Renal Denervation Reduced the Pulmonary Vascular Remodeling**

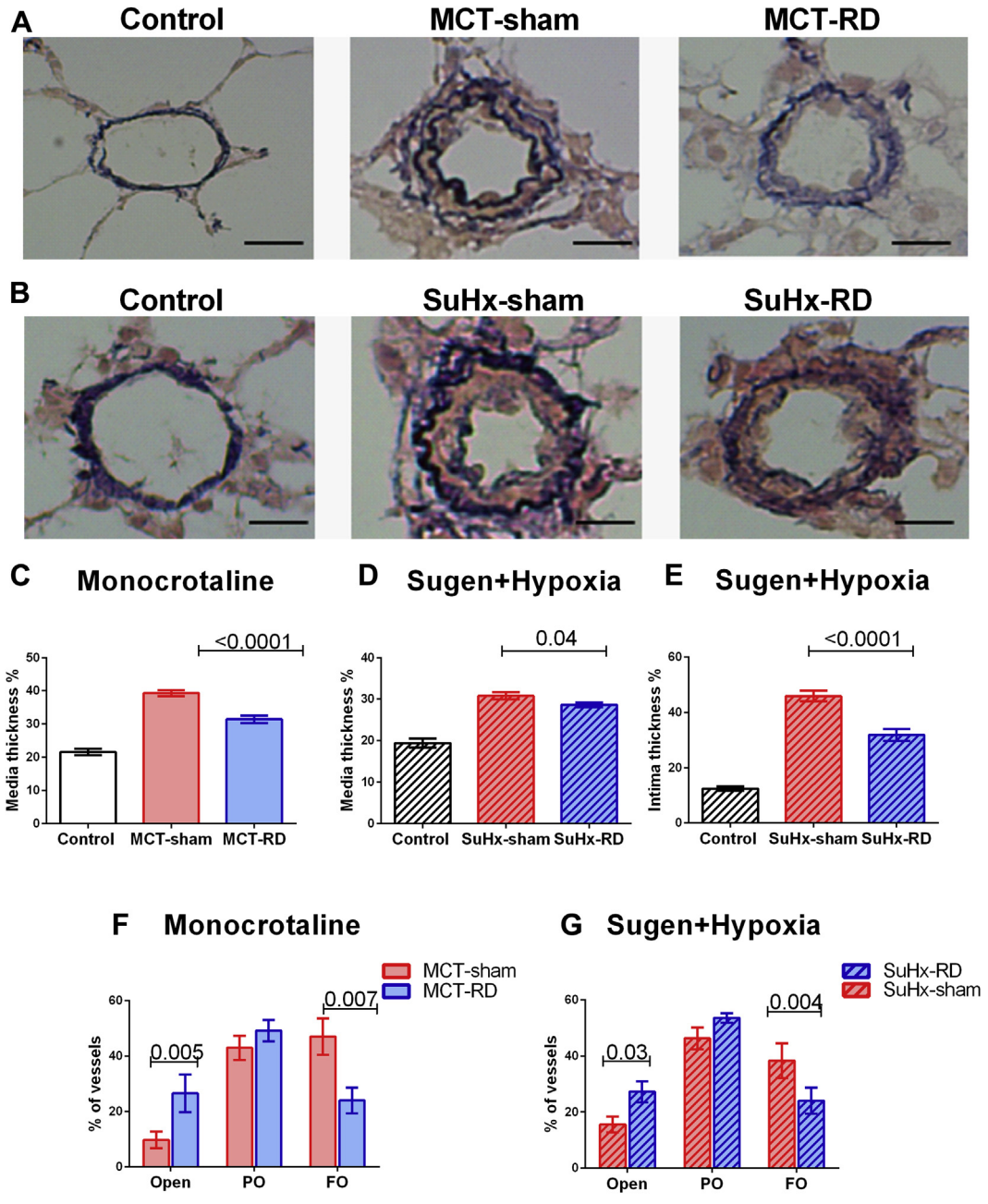

Representative examples of pulmonary arterioles (Elastica van Gieson) (scale bar, 20 μm). **(A)** Examples from the MCT model. **(B)** Examples from the SuHx model. RD reduced significantly the wall thickness of the pulmonary arterioles, as observed by a reduction in both the media (**C:** MCT; **D:** SuHx), and intima layers (**E:** SuHx). In addition, RD increased significantly the percentage of open vessels and reduced the number of full obliterated vessels in both PH-models (**F:** MCT; **G:** SuHx). **A:** Control: n = 5, MCT-sham: n = 9, and MCT-RD: n = 9; **B:** Control: n = 6, SuHx-sham: n = 10, and SuHx-RD: n = 10. Data are presented as mean ± SEM. Multilevel analysis to correct for non-independence of successive measurements per animal. FO = fully obliterated vessels; PO = partially obliterated vessels; other abbreviations as in Figure 1.

FIGURE 5 Renal Denervation Reduced Right Ventricular Hypertrophy and Fibrosis

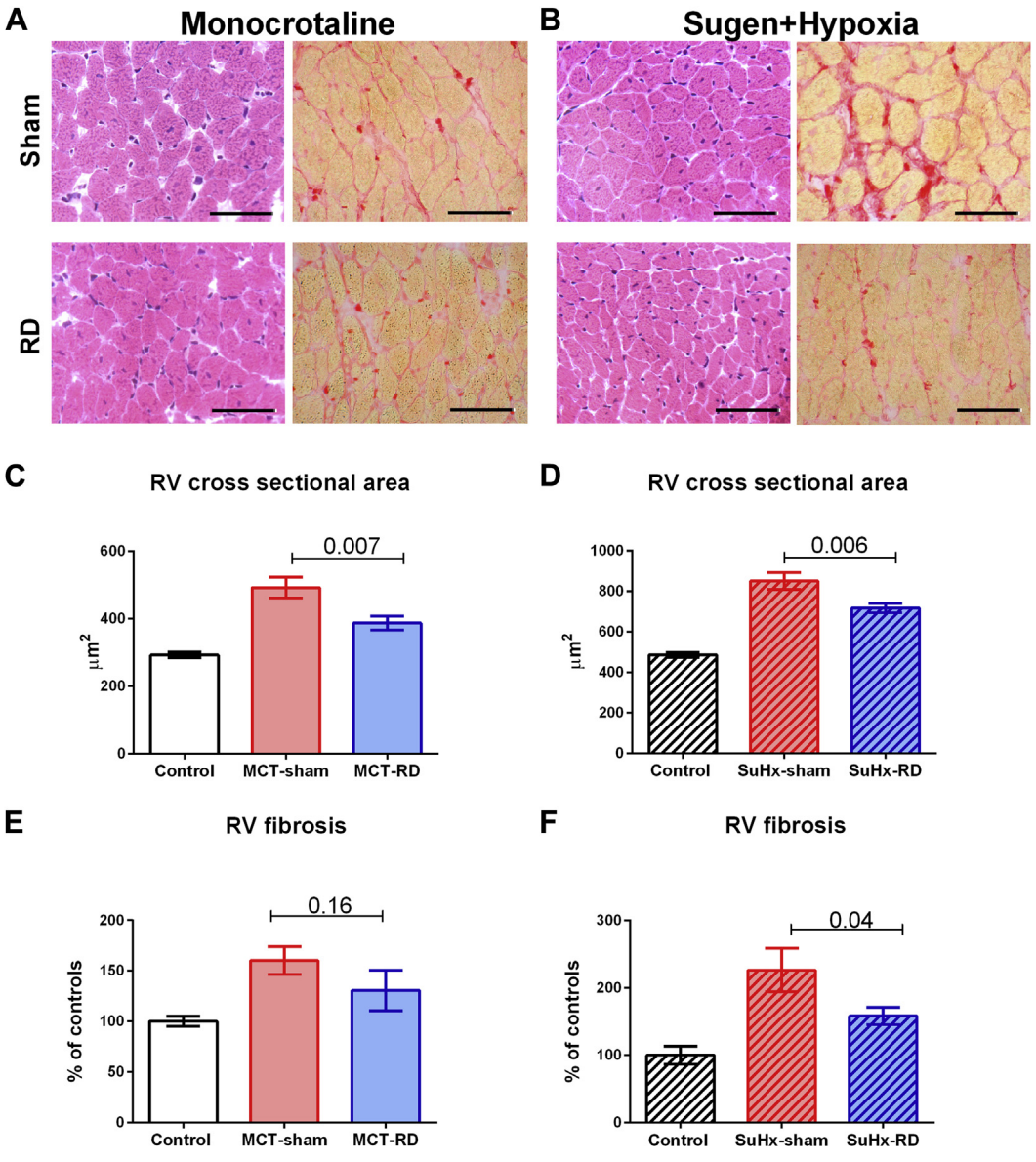

Representative examples of RV cross-sectional area (hematoxylin and eosin stain) and fibrosis (Picrosirius red stain) (scale bar, 20 μm). **(A)** Examples from an MCT-treated animal. **(B)** Examples from a SuHx model. RD reduced significantly the RV cross-sectional area (**C**: MCT; **D**: SuHx). RD reduced the RV fibrosis, especially in the SuHx-model (**E:** MCT; **F:** SuHx). **Right side:** Control: n = 5, MCT-sham: n = 9, and MCT-RD: n = 9. **Left side:** Control: n = 6, SuHx-sham: n = 10, and SuHx-RD: n = 10. Data are presented as mean ± SEM. Multilevel analysis has been performed to correct for non-independence of successive measurements per animal. Abbreviations as in Figure 1.

AT1 receptor density and the rate of proliferative cells. These data suggest that the beneficial effect of RD on pulmonary vascular remodeling could be partly explained by reduced AT1 receptor expression in PH rats. This is further supported by the observation that the results of RD are very similar to the previous reported effects of the angiotensin receptor blocker (losartan) in the MCT model (4), but not to the previous reported effects of beta-blockade (bisoprolol) (13). Nevertheless, the exact mechanisms by which RD improved the pulmonary vascular remodeling and RV diastolic stiffness in PH remain unclear.

FIGURE 6 Angiotensin II Type 1 Receptor and Mineralocorticoid Density in the Pulmonary Vasculature

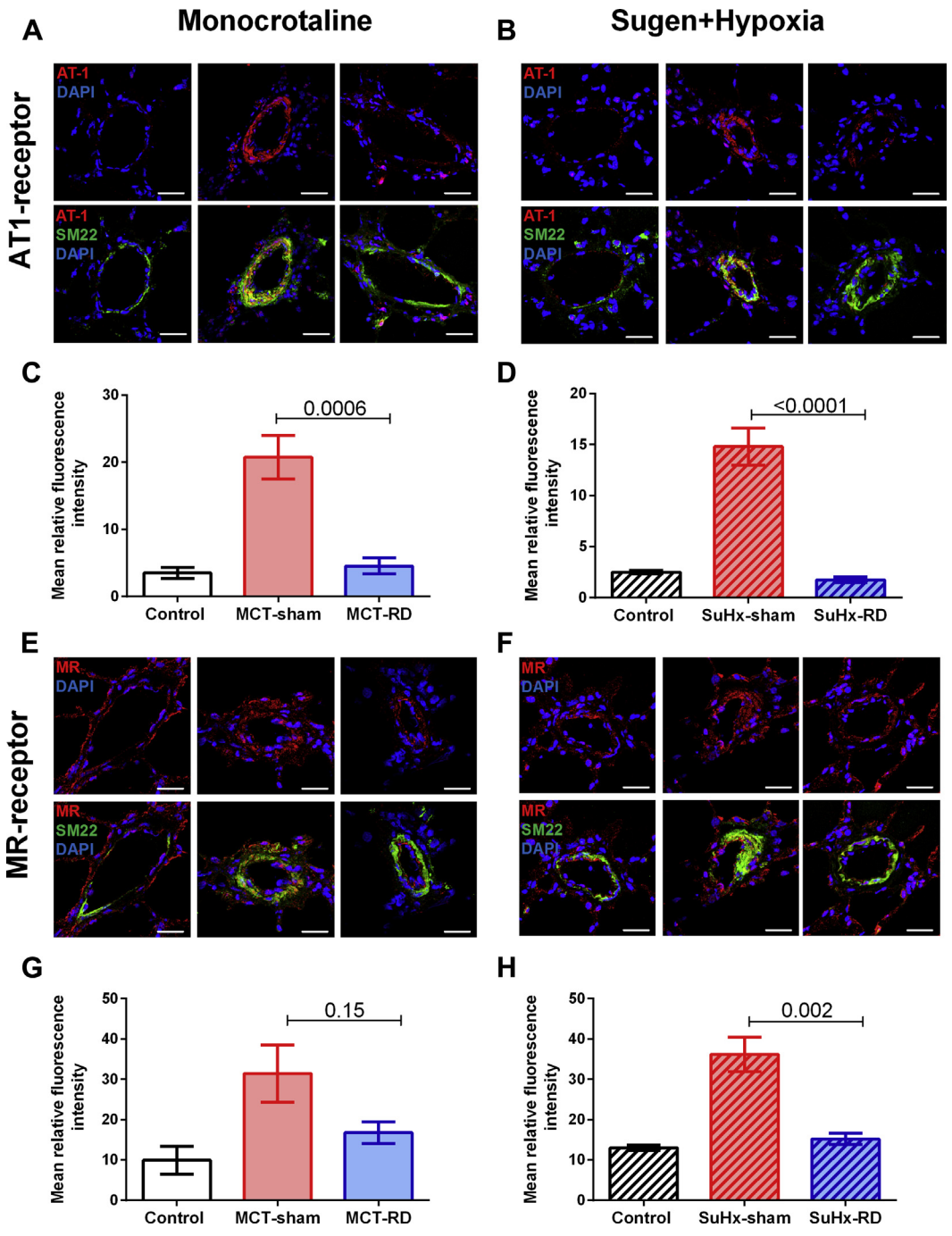

Representative images for AT1-receptor and MR-receptor immunofluorescence staining. **(A)** Examples from the MCT animal model. **(B)** Examples from the SuHx model. AT1-receptor **(red),** smooth muscle cells (SM22) **(green),** and nuclei (DAPI) (scale bar, 20 μm). **(C and D)** RD reduced AT1-receptor density in the pulmonary vasculature. **(E)** Examples from the MCT animal model. **(F)** Examples from the SuHx model: MR-receptor **(red),** SM22 **(green),** and nuclei (DAPI) (scale bar, 20 μm). **(G and H)** RD reduced MR-receptor density in the pulmonary vasculature in the SuHx-model. Control: n = 4, MCT-sham: n = 4, and MCT-RD: n = 4. Control: n = 4, SuHx-sham: n = 4, and SuHx-RD: n = 4. Data are presented as mean ± SEM. One-way ANOVA followed by Bonferroni correction. AT1= angiotensin II type 1 receptor; DAPI = 4′,6-diamidino-2-phenylindole; MR = mineralocorticoid receptor; SM = smooth muscle; other abbreviations as in Figure 1.

FIGURE 7 Proliferation Activity in the Pulmonary Vasculature

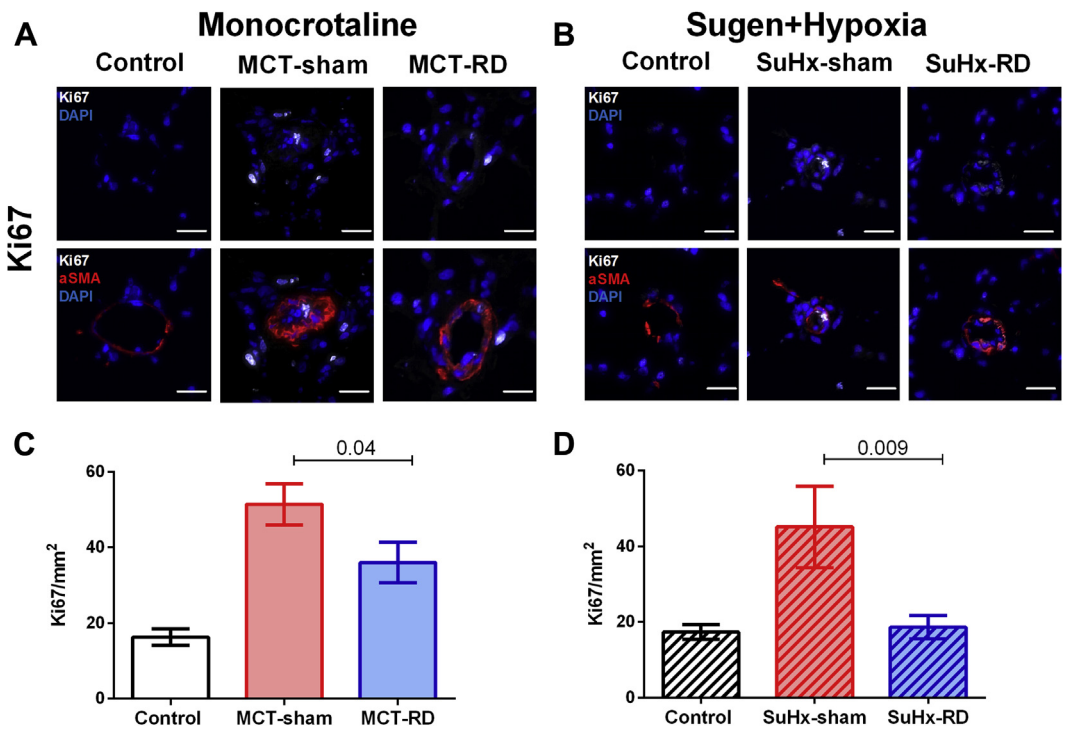

Representative images for Ki67 immunofluorescence staining. **(A)** Examples from the MCT animal model. **(B)** Examples from the SuHx model. Ki67 **(white),** α-smooth muscle actin **(red),** nuclei (DAPI) (scale bar, 20 μm). **(C and D)** RD reduced the proliferation in the pulmonary vasculature. Control: n = 4, MCT-sham: n = 5, and MCT-RD: n = 4. Control: n = 4, SuHx-sham: n = 4, and SuHx-RD: n = 4. Data are presented as mean ± SEM. One-way ANOVA followed by Bonferroni correction. Ki67 = cell proliferation marker; other abbreviations as in Figures 1 and 6.

In this proof-of-concept study, we provided some evidence that RD therapy in experimental PH may have some suppressive effect on RAAS. Despite the effects of RD on the RAAS, RD may also have effects on the SNS, which should be further explored in the PH context.

RD REDUCED RV DIASTOLIC STIFFNESS. Previous studies in resistant hypertensive patients have shown that catheter-based RD reduced LV hypertrophy and improved LV diastolic function independently of blood pressure and heart rate reduction (34-36). Furthermore, experimental studies in hypertensive and chronic pressure overload rat models demonstrated that RD was able to ameliorate LV maladaptive remodeling (37,38).

In the current study, we provide evidence that RD improved RV diastolic stiffness and RV remodeling in PH rats. We observed no significant changes in RV relaxation (dP/dt min, Tau), which do not necessarily correlate with RV stiffness (39).

Recently, we demonstrated that in severe PH, in addition to the myofibril stiffness, fibrosis also contributed to increase RV diastolic stiffness (40). One of the contributors of cardiac fibrosis and hypertrophy is the activation of MR, which could be mediated via aldosterone. Until now, little is known about the contribution of aldosterone activity and MR receptor on RV function and remodeling in PH. Important observations from Maron et al. (10,41) previously showed that aldosterone serum levels were increased in PH patients, as well as animal models of PH, and these levels were associated with cardiac dysfunction. In this study we observed increased expression of the MR receptor in the right ventricle of PH in comparison to control. In addition, RD was able to restore MR receptor expression, suggesting that RD could improve RV diastolic stiffness by reducing RV fibrosis via MR restoration in the RV.

STUDY LIMITATIONS. Although neurohormonal inhibitors may have some efficacy in experimental PH (4,42), their side effects may hamper their clinical translation. In this proof-of-concept study, we demonstrated that neurohormonal inhibition by

FIGURE 8 Angiotensin II Type 1 Receptor and Mineralocorticoid Receptor Expression in Right Ventricle Tissue

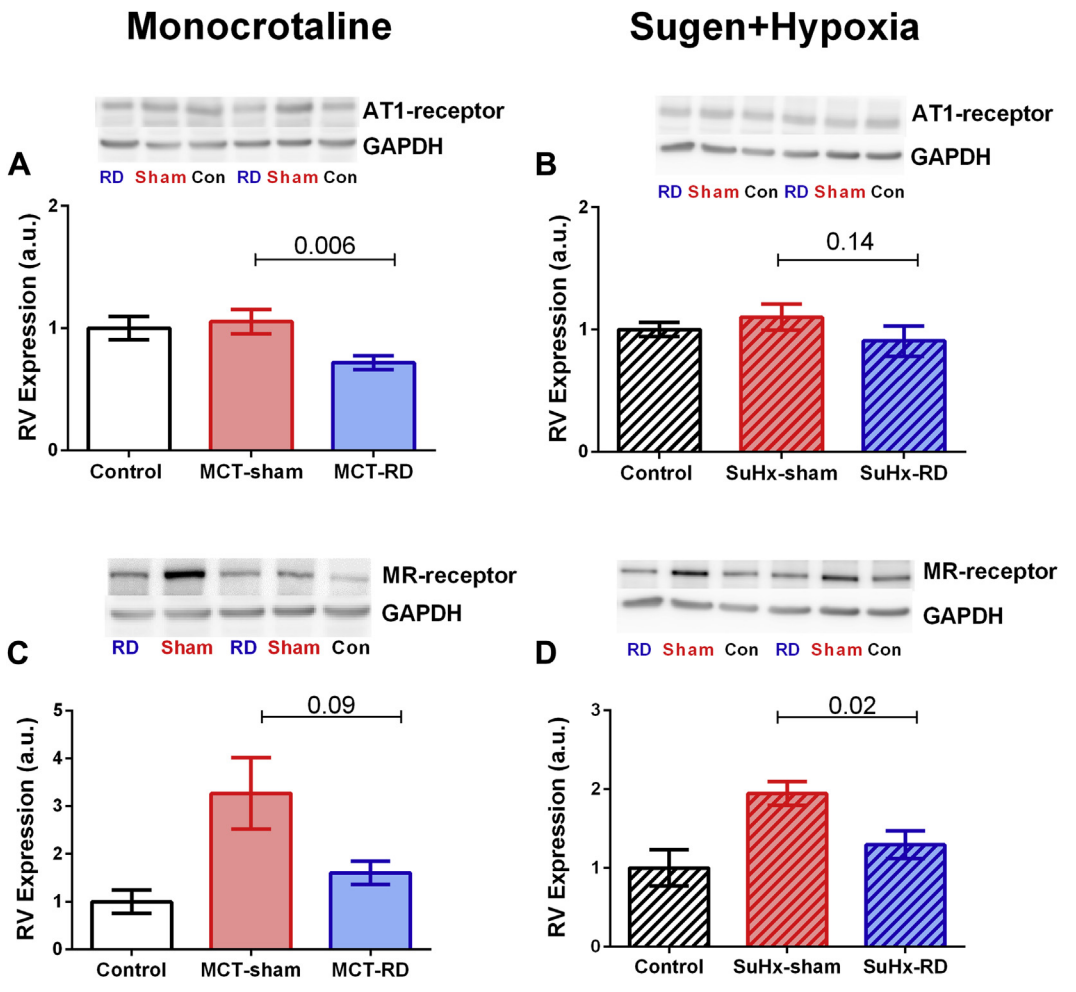

(A) Western blot analyses revealed significant reduction of AT1-receptor expression in the RV homogenates after RD in the MCT model in comparison to the sham-group. **(B)** However, no significant reduction was found in AT1-receptor expression in the SuHx model. **(C and D)** After RD, Western blot analyses revealed a significant reduction in the expression of MR-receptor in the SuHx-model. Protein expression was normalized by GAPDH, as a loading control. **On right side:** Control: n = 5, MCT-sham: n = 7, MCT-RD: n = 9; **on the left side:** Control: n = 6, SuHx-sham: n = 8 and SuHx-RD: n = 8. Data are presented as mean ± SEM. One-way ANOVA followed by Bonferroni correction. GAPDH = glyceraldehyde 3-phosphate dehydrogenase; other abbreviations as in Figures 1 and 6.

surgical RD was able to improve the pulmonary vascular remodeling and RV diastolic stiffness in 2 PH animal models, but this coincided with a decrease in systemic blood pressure. Although no other signs of discomfort were noticed, the finding of systemic hypotension is alarming and may limit the clinical translation of RD in clinical PH.

One limitation of our pressure-volume analyses is that we cannot obtain the absolute end-systolic/-diastolic volumes; therefore, some parameters cannot be estimated (e.g., the pressure-volume loop intercept, V0). However, the reported PV-derived parameters Ees, Eed, and Ea only rely on absolute changes in volumes, and do not depend on absolute volume measurements. Finally, we cannot exclude the possibility that renal denervation may have resulted in a small but clinically relevant increase in RV end-diastolic volume that we were not able to detect by echocardiography.

CONCLUSIONS

Using 2 well-established PH animal models, we provided evidence that chronic RD treatment delayed

disease progression. RD reduced pulmonary vascular resistance, RV afterload, pulmonary vascular remodeling, and RV diastolic stiffness. These beneficial effects could be associated with a partial suppression of RAAS after RD, as revealed by both a down-regulation of AT1 receptors in the pulmonary vasculature and a reduction of MR expression in RV homogenates.

ACKNOWLEDGMENTS The authors thank M. de Raaf, K. Kramer, C. Prins, H. van der Laan, and JP. Middelberg (VU University Medical Center, Amsterdam, the Netherlands) for their assistance and expertise.

ADDRESS FOR CORRESPONDENCE: Dr. M. Louis Handoko, Department of Cardiology, VU University Medical Center, De Boelelaan 1117, 1081 HV Amsterdam, the Netherlands. E-mail: ml.handoko@vumc.nl.

PERSPECTIVES

COMPETENCY IN MEDICAL KNOWLEDGE: Neurohormonal overactivation (increased SNS and renin angiotensin-aldosterone activity) plays an important role in the progression of pulmonary arterial hypertension. RD may be a promising therapy to reduce neurohormonal overactivation and delay PH progression.

TRANSLATIONAL OUTLOOK: Inhibition of neurohormonal activity by RD improved pulmonary vascular remodeling and RV diastolic stiffness in 2 PH animal models, but this was coincided with a decrease in systemic blood pressure. Although no other signs of discomfort were noticed, the finding of systemic hypotension is alarming and may limit the clinical translation of RD in clinical PH.

REFERENCES

1. Handoko ML, de Man FS, Allaart CP, Paulus WJ, Westerhof N, Vonk-Noordegraaf A. Perspectives on novel therapeutic strategies for right heart failure in pulmonary arterial hypertension: lessons from the left heart. Eur Respir Rev 2010;19:72–82.

2. Rain S, Handoko ML, Vonk Noordegraaf A, Bogaard HJ, van der Velden J, de Man FS. Pressure-overload-induced right heart failure. Pflugers Arch 2014;466:1055–63.

3. de Man FS, Handoko ML, Guignabert C, Bogaard HJ, Vonk-Noordegraaf A. Neurohormonal axis in patients with pulmonary arterial hypertension: friend or foe? Am J Respir Crit Care Med 2013;187:14–9.

4. de Man FS, Tu L, Handoko ML, et al. Dysregulated renin-angiotensin-aldosterone system contributes to pulmonary arterial hypertension. Am J Respir Crit Care Med 2012;186:780–9.

5. Maron BA, Leopold JA. Emerging concepts in the molecular basis of pulmonary arterial hypertension: part II: neurohormonal signaling contributes to the pulmonary vascular and right ventricular pathophenotype of pulmonary arterial hypertension. Circulation 2015;131:2079–91.

6. Maron BA, Leopold JA. The role of the renin-angiotensin-aldosterone system in the pathobiology of pulmonary arterial hypertension (2013 Grover Conference series). Pulm Circ 2014;4:200–10.

7. Velez-Roa S, Ciarka A, Najem B, Vachiery JL, Naeije R, van de Borne P. Increased sympathetic nerve activity in pulmonary artery hypertension. Circulation 2004;110:1308–12.

8. Wensel R, Jilek C, Dorr M, et al. Impaired cardiac autonomic control relates to disease severity in pulmonary hypertension. Eur Respir J 2009;34:895–901.

9. Ciarka A, Doan V, Velez-Roa S, Naeije R, van de Borne P. Prognostic significance of sympathetic nervous system activation in pulmonary arterial hypertension. Am J Respir Crit Care Med 2010:1269–75.

10. Maron BA, Opotowsky AR, Landzberg MJ, Loscalzo J, Waxman AB, Leopold JA. Plasma aldosterone levels are elevated in patients with pulmonary arterial hypertension in the absence of left ventricular heart failure: a pilot study. Eur J Heart Fail 2013;15:277–83.

11. Orte C, Polak JM, Haworth SG, Yacoub MH, Morrell NW. Expression of pulmonary vascular angiotensin-converting enzyme in primary and secondary plexiform pulmonary hypertension. J Pathol 2000;192:379–84.

12. Bogaard HJ, Natarajan R, Mizuno S, et al. Adrenergic receptor blockade reverses right heart remodeling and dysfunction in pulmonary hypertensive rats. Am J Respir Crit Care Med 2010;182:652–60.

13. de Man FS, Handoko ML, van Ballegoij JJ, et al. Bisoprolol delays progression towards right heart failure in experimental pulmonary hypertension. Circ Heart Fail 2012;5:97–105.

14. Perros F, Ranchoux B, Izikki M, et al. Nebivolol for improving endothelial dysfunction, pulmonary vascular remodeling, and right heart function in pulmonary hypertension. J Am Coll Cardiol 2015;65:668–80.

15. Singh JP, Kandala J, Camm AJ. Non-pharmacological modulation of the autonomic tone to treat heart failure. Eur Heart J 2014;35:77–85.

16. Bohm M, Linz D, Ukena C, Esler M, Mahfoud F. Renal denervation for the treatment of cardiovascular high risk-hypertension or beyond? Circ Res 2014;115:400–9.

17. Bohm M, Linz D, Urban D, Mahfoud F, Ukena C. Renal sympathetic denervation: applications in hypertension and beyond. Nat Rev Cardiol 2013;10:465–76.

18. Fong MW, Shavelle D, Weaver FA, Nadim MK. Renal denervation in heart failure. Curr Hypertens Rep 2015;17:17.

19. Stella A, Zanchetti A. Functional role of renal afferents. Physiol Rev 1991;71:659–82.

20. Kirchheim H, Ehmke H, Persson P. Sympathetic modulation of renal hemodynamics, renin release and sodium excretion. Klin Wochenschr 1989;67:858–64.

21. DiBona GF. Physiology in perspective: the Wisdom of the Body. Neural control of the kidney. Am J Physiol Regul Integr Comp Physiol 2005;289:R633–41.

22. Handoko ML, de Man FS, Happe CM, et al. Opposite effects of training in rats with stable and progressive pulmonary hypertension. Circulation 2009;120:42–9.

23. de Raaf MA, Schalij I, Gomez-Arroyo J, et al. SuHx rat model: partly reversible pulmonary hypertension and progressive intima obstruction. Eur Respir J 2014;44:160–8.

24. Hart EC, McBryde FD, Burchell AE, et al. Translational examination of changes in baroreflex function after renal denervation in hypertensive rats and humans. Hypertension 2013;62:533–41.

25. Brimioulle S, Wauthy P, Ewalenko P, et al. Single-beat estimation of right ventricular end-systolic pressure-volume relationship. Am J Physiol Heart Circ Physiol 2003;284:H1625–30.

26. Suga H, Sagawa K, Shoukas AA. Load independence of the instantaneous pressure-volume ratio of the canine left ventricle and effects of epinephrine and heart rate on the ratio. Circ Res 1973;32:314–22.

27. Hadi AM, Mouchaers KT, Schalij I, et al. Rapid quantification of myocardial fibrosis: a new macro-based automated analysis. Cell Oncol (Dordr) 2011;34:343–54.

28. De Man F, Handoko M, Groepenhoff H, et al. Effects of exercise training in patients with idiopathic pulmonary arterial hypertension. Eur Resp J 2009;34:669.

29. Rain S, Handoko ML, Trip P, et al. Right ventricular diastolic impairment in patients with pulmonary arterial hypertension. Circulation 2013; 128:2016–25.

30. Donazzan L, Mahfoud F, Ewen S, et al. Effects of catheter-based renal denervation on cardiac sympathetic activity and innervation in patients with resistant hypertension. Clin Res Cardiol 2015;105:364–71.

31. Dai Q, Lu J, Wang B, Ma G. Effect of percutaneous renal sympathetic nerve radiofrequency ablation in patients with severe heart failure. Int J Clin Exp Med 2015;8:9779–85.

32. Qingyan Z, Xuejun J, Yanhong T, et al. Beneficial effects of renal denervation on pulmonary vascular remodeling in experimental pulmonary artery hypertension. Rev Esp Cardiol (Engl Ed) 2015;68:562–70.

33. Santos-Gallego CG, Badimon JJ. Catheter-based renal denervation as a treatment for pulmonary hypertension: hope or hype? Rev Esp Cardiol (Engl Ed) 2015;68:551–3.

34. Schirmer SH, Sayed MM, Reil JC, et al. Improvements in left ventricular hypertrophy and diastolic function following renal denervation: effects beyond blood pressure and heart rate reduction. J Am Coll Cardiol 2014;63: 1916–23.

35. Brandt MC, Mahfoud F, Reda S, et al. Renal sympathetic denervation reduces left ventricular hypertrophy and improves cardiac function in patients with resistant hypertension. J Am Coll Cardiol 2012;59:901–9.

36. Tsioufis C, Papademetriou V, Dimitriadis K, et al. Effects of multielectrode renal denervation on cardiac and neurohumoral adaptations in resistant hypertension with cardiac hypertrophy: an EnligHTN I substudy. J Hypertens 2015;33:346–53.

37. Watanabe H, Iwanaga Y, Miyaji Y, Yamamoto H, Miyazaki S. Renal denervation mitigates cardiac remodeling and renal damage in Dahl rats: a comparison with beta-receptor blockade. Hypertens Res 2015;39:217–26.

38. Li ZZ, Jiang H, Chen D, et al. Renal sympathetic denervation improves cardiac dysfunction in rats with chronic pressure overload. Physiol Res 2015;64:653–62.

39. Kasner M, Sinning D, Burkhoff D, Tschope C. Diastolic pressure-volume quotient (DPVQ) as a novel echocardiographic index for estimation of LV stiffness in HFpEF. Clin Res Cardiol 2015;104: 955–63.

40. Rain S, Andersen S, Najafi A, et al. Right ventricular myocardial stiffness in experimental pulmonary arterial hypertension: relative contribution of fibrosis and myofibril stiffness. Circ Heart Fail 2016;9:e002636.

41. Maron BA, Zhang YY, White K, et al. Aldosterone inactivates the endothelin-B receptor via a cysteinyl thiol redox switch to decrease pulmonary endothelial nitric oxide levels and modulate pulmonary arterial hypertension. Circulation 2012;126:963–74.

42. Preston IR, Sagliani KD, Warburton RR, Hill NS, Fanburg BL, Jaffe IZ. Mineralocorticoid receptor antagonism attenuates experimental pulmonary hypertension. Am J Physiol Lung Cell Mol Physiol 2013;304:L678–88.

KEY WORDS **pulmonary hypertension, renin angiotensin system, right ventricular failure, sympathetic nervous system**

APPENDIX **For supplemental figures, text, tables, and references, please see the online version of this article.**